Features of superexchange nonresonant tunneling conductance in anchored molecular wires

Cite as: AIP Advances **9**, 115120 (2019); https://doi.org/10.1063/1.5124386
Submitted: 13 August 2019 . Accepted: 05 November 2019 . Published Online: 25 November 2019

Elmar G. Petrov, Yevgen V. Shevchenko, Vladislav Snitsarev, Victor V. Gorbach, Andrey V. Ragulya, and Svetlana Lyubchik

Features of superexchange nonresonant tunneling conductance in anchored molecular wires

Cite as: AIP Advances 9, 115120 (2019); doi: 10.1063/1.5124386
Submitted: 13 August 2019 • Accepted: 5 November 2019 •
Published Online: 25 November 2019

Elmar G. Petrov,[1,a)] Yevgen V. Shevchenko,[1] Vladislav Snitsarev,[2] Victor V. Gorbach,[3] Andrey V. Ragulya,[3] and Svetlana Lyubchik[4,5]

AFFILIATIONS

[1]Bogolyubov Institute for Theoretical Physics, National Academy of Sciences of Ukraine, Kiev UA-03680, Ukraine
[2]Montclair State University, Montclair, New Jersey 07043, USA
[3]Nanotechcenter LLC, Kiev 03142, Ukraine
[4]REQUIMTE, Departomento Quimica, FCT, Universidade Nova de Lisboa, Caparica 2829-516, Portugal
[5]Faculdade de Engenharias, Universidade Lusofona de Humanidades e Tecnologias, Lisboa 1749-024, Portugal

[a)]**Electronic mail:** epetrov@bitp.kiev.ua

ABSTRACT

A modified superexchange model is used to clarify the physical mechanisms for the formation of nonresonant tunneling conductance in terminated molecular wires. Due to the specific relationship between its key parameters, this model has wider areas of applicability compared to the flat-barrier model and the standard superexchange model, which are widely involved for the physical interpretation of experimental results. Moreover, the results obtained in the two latest models appear in the modified model as characteristic limiting cases. Our estimates show that the exponential decay of conductance, characterized by an attenuation factor β (per repeating unit), is limited by the conditions $\beta \leq 1.2$ and $\beta \geq 3.7$ for the flat-barrier and standard models, respectively. At the same time, the modified superexchange model yields $\beta > 0$, which, thus, allows us to analyze the tunneling conductance in molecular wires containing both saturated and conjugated bonds. We also show that for a small number of N repeating wire units (about 3–6 depending on the value of β), the exponential dependence of conductance on N is violated and, accordingly, contact conductance is not identical to conductance at $N = 0$. Formulas are found which, on the basis of experimental data, make it possible to establish the values of superexchange parameters as well as indicate the conditions of possible hybridization between the orbitals of the anchor groups and the adjacent end units belonging to the interior wire region. One example is the establishment of features in the tunneling conductance of terminated alkane chains caused by the nature of their anchor groups.

I. INTRODUCTION

The use of organic molecules for the nanoscale devices is one of the promising directions in miniaturization of electronic, optoelectronic, and spintronic circuit components.[1–8] Here, significant progress has been achieved by applying scanning tunneling and atomic force microscopes for monitoring and controlling the charge transfer processes in molecular junctions as well as for the fabrication of molecular structures with desirable conduction properties.[9,10] The molecular junctions where single molecules or self-assembled monolayers are embedded between the electrodes can fulfill the functions of molecular wires, diodes, transistors, registers, switches, etc.[11–15] A number of factors, such as the molecule-electrode couplings, the energy position of molecular orbitals (MOs) relative to the Fermi-levels, electronic density of states, molecular conformation and configuration mobility, etc., control the current-voltage and conductance characteristics of single molecules and molecular structures.[7,16] Therefore, the efficiency of charge transmission pathways depends strongly on the type of the molecular junction as well as the magnitude and polarity of the applied electric field.

One of the fundamental processes that manifest themselves in nanoscale physics is the tunneling of charges (electrons/holes) through individual molecular wires. A typical molecular wire is a regular chain of repeating monomers, where the end monomers are attached to terminal units. The latter play an important role in the formation of stable self-assemble monolayers and the specific circuits for molecular devices.[3,7,13,17,18] Numerous experiments on the study of the tunneling processes in molecular wires embedded between the metal electrodes show an exponential decrease in conductance g with the number N of repeating chain units,[19–21] i.e., $g \simeq A\exp(-\beta N)$. The pre-exponential factor A reflects a contact of the wire with the electrodes and thereby determines the efficiency of the tunneling penetration of electrons/holes to the molecular wire and their tunneling departure from the wire. As for the attenuation factor β, it represents the features of the formation of coherent charge transfer through a regular chain (interior range of the wire).

The clarification of physical mechanisms responsible for the formation of factors A and β is one of the most important problems in the electronics of nanoscale transport processes. The ideal way is to calculate the conductance based on first principles. However, due to the complexity of the metal-molecular wire-metal system, this method encounters significant difficulties. Nevertheless, based on the theory of complex band structures for long chains with repeating monomers,[22] it was possible to obtain the value of β-factor close to that observed in the experiment.[22–25] It is much more difficult to find from the first principles, the numerical values of factor A. This is due to the variations in binding geometry of anchor groups to the adjacent electrodes.[20,26,27]

The analysis of experimental data is mainly carried out using the analytical formulas obtained with the use of one or another physical model. To study the dependence of the conductance of the molecular wire on its length, the most popular are the Simmons barrier model[28] and the McConnell superexchange model.[29] Both allow us to express the factors A and β through the parameters attributed to the model. However, serious difficulties arise in the choice of physically validated parameters. For example, in the Simmons model, the problem exists with fitting the height of a tunneling barrier.[19,30–34] As for the McConnell model, it works in deep tunneling mode.[35–38] Thus, there is a need to use such a model that would allow us to obtain analytical formulas with clearly defined areas of applicability, and in particular cases, these formulas would correspond to those that follow from the Simmons and McConnell models. For this purpose, it is proposed to use a modified superexchange model, which is a generalization of the standard superexchange model. The generalization consists in removing restrictions on the relationship between the key parameters characterizing the superexchange within the interior wire region—a chain of repeating units.

In this paper, the potentialities of a modified superexchange model are used to elucidate the physics of the formation of tunneling conductance of molecular wires of various lengths and with different types of anchor groups that bind the wire to the electrodes.[7,16,39] As an example, we applied the theory to the analysis of experimental data related to the tunneling conductance of symmetrical X–$(CH_2)_n$–X molecular wires, in which the n-alkane chains are attached to the electrodes through small anchoring groups X = SH, NH_2, and COOH.[26] Based on the results of the analysis, it was possible to identify the physical features of the tunneling transmission associated with both the alkane chain and anchoring groups that make physical and chemical contact with the electrodes. It was especially important to compare the attenuation factors obtained in the modified superexchange model with those used in the phenomenological Simmons's barrier model[19–21,30,40] or in McConnell's superexchange model.[19,41–45] This made it possible to significantly advance in understanding the mechanisms of control of electron-transport processes in molecular junctions.

This paper is organized as follows. In Sec. II, we obtain an analytic expression for nonresonant tunneling conductance in a terminated molecular wire. Section III analyzes the results of experiments and gives their physical interpretation. A summation of the results of general physical significance is presented in Sec. IV.

II. MODEL AND BASIC EQUATIONS

For the convenience of the reader, Table I defines the basic values used in this paper.

We derive analytic formulas based on the rigorous Landauer-Büttiker integral expression for the current through nonmagnetic molecular junctions. In the absence of a magnetic field, the tunneling *electron current* across the molecular wire can be calculated with the following expression:[46,47]

$$I = \frac{|e|}{\pi\hbar}\int_{\mu_R}^{\mu_L} dE\, T(E,V), \tag{1}$$

where $|e|$ is the absolute electron charge and $T(E, V)$ is the wire transmission function at a voltage bias V. The use of chemical potentials μ_L and μ_R for the left (L) and right (R) electrodes as the integration limits suggests that the contribution to the current is mainly due to electrons that leave occupied levels (positioned below the Fermi level of one of the electrodes) and arrive to empty levels (positioned above the Fermi level of another electrode). This situation is well implemented at temperatures below room temperature (see Ref. 48 in more detail). The transmission function reads $T(E,V) = tr\left[G(E)\Gamma_L(E)G^{+}(E)\Gamma_R(E)\right]$, where $G(E) = I/(EI - H)$ is the Green's operator, with E, I, and $H = H_W + \Sigma_L(E) + \Sigma_R(E)$ being the tunneling energy, the unit operator, and the effective wire Hamiltonian, respectively. The latter includes the wire Hamiltonian H_W (in the absence of interaction between the wire and the electrodes) and the self-energy operators $\Sigma_{L(R)}(E)$ generated by the interaction of the wire with the electrodes. The self-energy operators also determine the width operators $\Gamma_r(E) = 2\,\mathrm{Im}\Sigma_r(E)$.

A. Tight-binding approach

To specify the superexchange model, we employ the tight-binding version of the electron-transfer process, which is widely used to study a long-range interelectrode electron transfer mediated by the bridging molecular chains.[35,49–54] Let $k = 0$, $N + 1$, and $k = 1, 2, \ldots, N$ denote the terminal and interior wire units, respectively. Assuming an analysis of the experimental data related to the nonresonant conductance of a symmetric molecular wire embedded between the identical electrodes, we represent the effective wire

TABLE I. List of main variables utilized in this paper.

Symbol	Meaning
μ_L, μ_R	Chemical potentials
$i_0(g_0)$	Current (conductance) unit
β_N	Attenuation factor (per chain unit)
$l_c(l_*)$	Distance from a terminal unit to the surface site (edge chain unit), Fig. 1
l_s	Distance between neighboring chain units, Fig. 1
t_s	Coupling between neighboring C–C bonds, Fig. 1
T_*	Coupling between terminal and adjacent chain units, Fig. 1
$E_*(\eta_c)$	Voltage division factor for terminal units (center of delocalized electron density)
$E_c(E_s)$	Energy position of the biased (unbiased) center of delocalized electron density, Fig. 2
E_H	Energy position of the HOMO for a long chain, Fig. 2
$\Delta E_{Ls}, \Delta E_{Rs}$	Principal transmission gaps, Fig. 2 and Eq. (12)
ΔE_s	Unbiased principal transmission gap
$\Delta E_{r0}, \Delta E_{rN+1}$	Terminal transmission gaps, Eq. (19)
ΔE	Apparent tunneling barrier, Fig. 2
$\Delta E_0 = \Delta E_{\|V=0}$	Zero-bias tunneling barrier
ΔE_*	Unbiased gaps for terminal units $k = 0$ and $k = N + 1$
Γ_*	Broadening of orbital energy for terminal units $k = 0$ and $k = N + 1$
Γ_e	Zero-bias width factor, Eq. (5), for edge chain units $k = 1$ and $k = N$
λ_u	Contact factor in the wire with identical terminal units X
g_u	Conductance of the wire with a single C–C bond and terminal units X

Hamiltonian in the form of the trigonal matrix,[35,49]

$$H = \begin{pmatrix} \mathscr{E}_0 & -t_* & 0\cdots & 0 \\ -t_* & E_1 & -t_s\cdots & 0 \\ \vdots & \vdots & \ddots & \vdots \\ 0\cdots & -t_s & E_N & -t_* \\ 0 & \cdots & -t_* & \mathscr{E}_{N+1} \end{pmatrix}. \tag{2}$$

Here, $t_* = -t_{01} = -t_{NN+1}(>0)$ and $t_s = -t_{kk+1}(>0)$ are the couplings between the neighboring sites of electron localization (cf. Fig. 1),

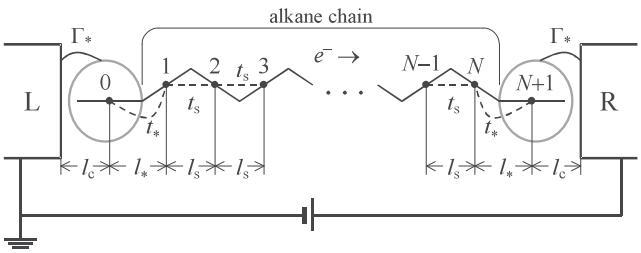

FIG. 1. Linear *n*-alkane chain attached to the left (L) and right (R) electrodes via the terminal units $k = 0$ and $k = N + 1$, respectively. The centers of electron localization on the interior wire units (here, the bonds C–Cσ) are denoted by $k = 1, 2, \ldots, N$. The distance between the neighboring centers is l_s. The center of electron localization at the terminal unit $0(N + 1)$ is separated from the edge C–C bond and the adjacent electrode surface by the distances l_* and l_c, respectively. Rest explanations are in the text.

whereas E_k and $\mathscr{E}_{0(N+1)} = E_{0(N+1)} - i\Gamma_*/2$ are the on-site energies of the kth interior and the $0(N + 1)$th terminal wire units, respectively. Quantity $\Gamma_* \equiv \Gamma_L = \Gamma_R$ is the width parameter characterizing the broadening of orbital energy of the terminal unit caused by interaction of the unit with the adjacent electrode. (Assuming electrodes with wide conduction bands, we neglect the dependence of the parameter Γ_* on E.) Now, following the method represented in Refs. 36, 49, and 54, one gets

$$T(E, V) = \Gamma_*^2 t_*^2 (-t_s)^{N-1} / \mathrm{Det}_{0N+1}(E), \tag{3}$$

where $\mathrm{Det}_{0N+1}(E)$ is the determinant of matrix $EI - H$. At a small mixture of terminal orbitals with interior wire orbitals, the determinant can be represented in the factorized form,[38] $\mathrm{Det}_{0N+1}(E) \approx (E - \mathscr{E}_0)(E - \mathscr{E}_{N+1}) \prod_{v=1}^{N} (E - \mathscr{E}_v)$. Here, $\mathscr{E}_{0(N+1)}$ is the above-mentioned on-site energy of the terminal unit, whereas $\mathscr{E}_v$ is the eigenvalue of the chain Hamiltonian H_{chain}, which is given by the diagonal and off-diagonal matrix elements $E_k\delta_{k',k}$ and $-t_s\delta_{k',k\pm1}$, respectively. The factorization yields

$$T(E, V) \simeq \Gamma_1(E - E_0)\Gamma_N(E - E_{N+1})|G_{1N}(E)|^2, \tag{4}$$

where

$$\Gamma_{1(N)}(\Delta) = 2\pi t_*^2 \mathscr{L}(\Delta), \quad \left(\mathscr{L}(\Delta) = \frac{1}{\pi} \frac{\Gamma_*/2}{\Delta^2 + \Gamma_*^2/4}\right) \tag{5}$$

can be treated as an edge width factor that determines the linker-mediated broadening of the orbital energy level of the $1(N)$th edge chain unit via both its coupling to the $0(N + 1)$th terminal unit (quantity t_*) and Lorentzian $\mathscr{L}(\Delta)$. The latter contains the

above-mentioned width parameter Γ_*. The value of the Γ_* strongly depends on the nature of the wire-electrode contact.[27,40,55,56] For instance, dependent on the contact geometry, one can fix the high and low tunneling conductance through one and the same alkane chain.[26,45] Quantity $G_{1N}(E) = (-t_s)^{N-1}\prod_{\nu=1}^{N}[1/(E-\mathscr{E}_\nu)]$ is the matrix element $\langle 1|G_{chain}(E)|N\rangle$ of chain's Green operator $G_{chain}(E) = I/(E - H_{chain})$. The value of $G_{1N}(E)$ reflects the superexchange between the edge units 1 and N of the regular chain mediated by $N-1$ bonds. In this paper, we consider the tunneling transmission, at which the voltage bias V does not destroy the delocalization of the MOs of a regular chain. It has been found[37,38] that in this case, the eigenvalue of the Hamiltonian H_{chain} has a standard form,

$$\mathscr{E}_\nu = E_c - 2t_s\cos[\pi\nu/(N+1)], \quad (\nu = 1, 2, \ldots, N). \tag{6}$$

Specificity is only in the value

$$E_c = E_s - |e|V\eta_c \tag{7}$$

that characterizes the Stark shift of zero-bias on-site energies $E_1^{(0)} = E_2^{(0)} = \cdots = E_N^{(0)} \equiv E_s$. The shift is governed by the voltage division factor $\eta_c = [l_* + l_c + l_s(N-1)/2]/l$ [$l = 2(l_c + l_*) + l_s(N-1)$ is the total interelectrode distance, Fig. 1]. Physically, in line with Eqs. (6) and (7), the E_c coincides with the energy position of the center of the delocalized electron density, which is uniformly distributed over all chain units. In the same approximation, such a delocalization cancels the ramp across the interior range of the wire so that the chain's on-site orbital energies remain equal to each other (i.e., $E_1 = E_2 = \cdots = E_N \equiv E_c$) and exhibit the identical Stark shift. This means that within the interior range of the wire, the ramp is replaced with a uniform electrostatic profile. A similar effect has been earlier noted in Refs. 37, 47, and 57. Quantity $\mathscr{E}_\nu$, Eq. (6), can be attributed to the energies of the delocalized chain HOMOs (i.e., HOMO = $\text{HOMO}_{\nu=N}$, HOMO−1 = $\text{HOMO}_{\nu=N-1}$, ...) or LUMOs (i.e., LUMO = $\text{LUMO}_{\nu=1}$, LUMO+1 = $\text{LUMO}_{\nu=2}$, ...). As was shown in Refs. 37 and 38, expression (6) retains its form and, therefore, the delocalization of MOs in a chain with repeating units is not destroyed by the voltage bias until condition

$$\zeta = |\Delta_s/2t_s|\,S(N) \ll 1 \tag{8}$$

is satisfied. In Eq. (8), $\Delta_s = |e|V\,(l_s/l)$ is the energy drop between the identical neighboring chain units caused by the bias and

$$S(N) = \left(\frac{1}{N+1}\right)\left[\frac{1}{1-\cos\left(\frac{\pi}{N+1}\right)} - \frac{1}{1-\cos\left(\frac{3\pi}{N+1}\right)}\right] \times \left[\frac{1}{\cos\left(\frac{\pi}{N+1}\right) - \cos\left(\frac{2\pi}{N+1}\right)}\right] \tag{9}$$

is the function that controls an impact of the chain length on the applicability of the model of the delocalized MOs even though $V \neq 0$. Its numerical values (Table II) are the same for any linear chain with one frontier orbital per chain unit. Inequality (8) specifies the conditions under which the uniform profile is preserved, and the energies of delocalized MOs are given by Eq. (6). Therefore, substituting the $\mathscr{E}_\nu$ from this expression into the $\prod_{\nu=1}^{N}[1/(E-\mathscr{E}_\nu)]$, one derives (see also Refs. 50 and 58)

$$G_{1N}(E) = (-1)^{N-1}t_s^{-1}\frac{\sinh[\beta(\varepsilon)/2]}{\sinh[(N+1)\beta(\varepsilon)/2]}. \tag{10}$$

TABLE II. Numerical values of function $S(N)$.

N	1	2	3	4	5	6	7
S		0.5	1	1.79	2.94	4.54	6.64
N	8	9	10	11	12	13	14
S	9.33	12.7	16.8	21.6	27.4	27.4	41.8
N	15	16	17	18	19	20	21
S	50.6	60.6	71.9	84.4	98.3	114	131

Here, the $\beta(\varepsilon)$ is defined by the relation $\cosh[\beta(\varepsilon)/2] = \varepsilon/2t_s$, in which $\varepsilon = |E - E_c|$ is the tunneling energy measured from the position of the E_c [cf. Eq. (7) and Fig. 2]. If the superexchange involves the HOMOs, then $\varepsilon = E - E_c > 0$.

B. Tunneling conductance

Substituting the factorized transmission function $T(E, V)$ given by Eqs. (3), (4), and (10) into the basic integral form (1), we arrive at the following expression for the tunneling current:

$$I = i_0\int_{\Delta E_{Rs}}^{\Delta E_{Ls}}\frac{d\varepsilon}{\varepsilon^2}\,\Gamma_1(\varepsilon - \Delta E_{0c})\Gamma_N(\varepsilon - \Delta E_{N+1c})\Phi(\beta(\varepsilon), N). \tag{11}$$

[Quantity $i_0 \equiv (|e|/\pi\hbar) \times 1\ \text{eV} \approx 77.4\ \mu\text{A}$ is the current unit.] In Eq. (11), the tunneling energy ε is restricted by the energy window, which is determined by principal transmission gaps $\Delta E_{L(R)s} = \mu_{L(R)} - E_c$ (cf. Fig. 2). In the case of a perfectly symmetric molecular wire (where $\eta_c = 1/2$), it reads

$$\Delta E_{rs} = \Delta E_s + (|e|V/2)\,(\delta_{r,L} - \delta_{r,R}), \tag{12}$$

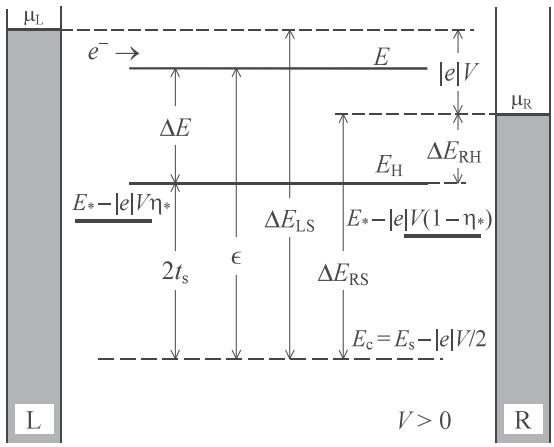

FIG. 2. Position of the transmission energy $\varepsilon = E - E_c$ with respect to the "center of gravity" of electronic density distributed over the delocalized HOMOs of the alkane chain. When tunneling energy E enters in energy window $\mu_L \geq E \geq \mu_R$, then the ε varies between the principal transmission gaps ΔE_{Rs} and ΔE_{Ls}. Quantity $\Delta E = E - E_H$ is the energy distance between tunneling energy and the HOMO level position $E_H = E_c - 2t_s$ for a long ($N \gg 1$) regular chain. When $E - E_H \ll 2t_s$, then quantity ΔE can be treated as the height of the rectangular barrier.

where $\Delta E_s = E_F - E_s$ is the unbiased gap [$E_F = \mu_{L(|V=0)} = \mu_{R(|V=0)}$ is the energy of the unbiased Fermi level]. The specific property of Eq. (11) is that the dependence of the integrand on V is contained only in the edge width factors $\Gamma_{1(N)}(\varepsilon - \Delta E_{0(N+1)c})$. In these factors, the energy differences $\Delta E_{0(N+1)} = E_{0(N+1)} - E_c$ determine the offsets of orbital energies of terminal units, $E_0 = E_* - |e|V\eta_*$ and $E_{N+1} = E_* - |e|V(1-\eta_*)$, with respect to the energy position of the center of delocalized electron density E_c (cf. Fig. 2). Quantity E_* is their zero-bias position, while $\eta_* = l_c/l$ is the terminal's voltage division factor. Main dependence of the conductance on the number of chain units N is concentrated in the chain attenuation function,

$$\Phi(\beta(\varepsilon), N) = \frac{\sinh^2 \beta(\varepsilon)}{\sinh^2 [(N+1)\beta(\varepsilon)/2]}, \tag{13}$$

which is equal to unity at $N = 1$ and, thus, is especially convenient for the quantitative description of superexchange decrease in the tunneling conductance with increasing number of repeating wire units.[37] Quantity

$$\beta(\varepsilon) = 2\ln\left[\varepsilon/2t_s + \sqrt{(\varepsilon/2t_s)^2 - 1}\right] \tag{14}$$

is the attenuation factor in the modified superexchange model. [In the standard superexchange model, we get $\beta(\varepsilon)$ in form (17) valid at condition (16); thus, the modification is that there is no restriction on the ratio $\varepsilon/2t_s$.]

Equations (11)–(14) are the basic to derive analytic expressions for the tunneling current and the conductance. At nonresonant tunneling, the $\beta(\varepsilon)$ is a real value if only

$$\varepsilon/2t_s > 1 \tag{15}$$

or, what is the same, $E > E_H = E_c + 2t_s$ (cf. Fig. 2). Note here that McConnell's superexchange model works at the condition

$$(\varepsilon/2t_s)^2 \gg 1 \tag{16}$$

and brings to attenuation factor in the form[35,36]

$$\beta(\varepsilon) = 2\ln(\varepsilon/t_s). \tag{17}$$

In this paper, the situation is considered at which the voltage bias is such that the orbital energies of terminal units remain below E_H and, thus, do not enter in the transmission window (ΔE_{Ls}, ΔE_{Rs}). Therefore, the edge width factors $\Gamma_{1(N)}(\varepsilon - \Delta E_{0(N+1)c})$ exhibit a weak dependence on V. As a result, for the conductance $g = \partial I/\partial V$, one derives

$$g \simeq \frac{g_0}{2} \sum_{r=L,R} \frac{\Gamma_1(\Delta E_{r0})\Gamma_N(\Delta E_{rN+1})}{\Delta E_{rs}^2} \Phi(\beta_r, N) \tag{18}$$

where $g_0 = |e|i_0 \approx 77.4\ \mu$S is the quantum unity conductance. The voltage dependence of the $g = g(V)$ is contained in principal transmission gaps ΔE_{rs}, Eq. (12), as well as in the terminal transmission gaps $\Delta E_{r0(N+1)} = \mu_r - E_{0(N+1)}$, which for symmetrical wires appear as

$$\begin{aligned} \Delta E_{r0} &= \Delta E_* + |e|V[\eta_* \delta_{r,L} - (1-\eta_*)\delta_{r,R}], \\ \Delta E_{rN+1} &= \Delta E_* - |e|V[\eta_* \delta_{r,R} - (1-\eta_*)\delta_{r,L}]. \end{aligned} \tag{19}$$

Here, $\Delta E_* = E_F - E_*$ is the unbiased terminal gap. In function $\Phi(\beta_r, N)$, the attenuation factor β_r is specified by Eq. (14), in which $\varepsilon = \Delta E_{rs}$.

III. RESULTS AND DISCUSSION

As an example of applying the theory to the analysis of experimental data, we considered nonresonant tunneling conductance in the terminated n-alkane chains. In line with quantum-mechanical calculations[8,59,60] and experimental data,[61] energy of the highest occupied molecular orbital (HOMO) of alkane chain is closer to the electrode's Fermi level compared to the energy of the lowest unoccupied molecular orbital (LUMO). Therefore, the tunneling conductance of the chain is mainly caused by the virtual departure of electrons from double-filled localized orbitals or, what is the same, the virtual arrival of holes in the same orbitals. There are many different superexchange pathways in alkanes.[62] Among them, the dominant pathway is associated with the overlap of the wave functions of the neighboring C–Cσ orbitals. This is supported by the fact that in the HOMO the electron density is concentrated mainly on $N(= n - 1)$ C–Cσ bonds.[8,59,60] (In the LUMO, the electron density is largely located at the C atoms.[8]) As to the terminal units, they are anchored to the electrodes through the groups SH, NH_2, and COOH. It is assumed that the lone pairs of atoms S, N, and O bind preferably to uncoordinated gold adatoms, thereby providing a coupling between the terminal wire units and the corresponding gold atoms.[63–66] The lone pairs of sulfur and nitrogen atoms can also form the hybrids with the surface gold atoms,[47,64] thus facilitating conductance of the wire. In the considered wires X–$(CH_2)_n$–X, the dominant superexchange pathway of coherent charge transfer is based on the virtual participation of localized orbitals belonging to terminal units, as well as the HOMOs, which mainly formed from C–Cσ bonds. Therefore, in the framework of the tight-binding picture of the tunneling process, the chain on-site energies E_k and the site-to-site couplings t_s are mainly associated with the C–Cσ bonds.[37,38,67] In accordance with the quantum-chemical calculations,[59,60] the couplings of lone pairs to the C–Cσ bonds do not have a significant effect on the electron density distribution along the alkane chain, and thus there is little mixing between the wave functions of the terminal units and the internal wire units (attributed to the alkane chain). This means that the condition for obtaining Eq. (11) is assumed to be fulfilled.

To clarify the physics of tunneling electron transmission in the terminated linear molecular chains, we compare theoretical results with experimental data on the low and high tunneling conductance of symmetrical molecular wires in which alkane chains were attached to gold electrodes using three types of anchor groups.[26] The experiment, which is analyzed in this paper, covers the ohmic tunneling and gives the numerical values of only two quantities, the near zero-bias pre-exponential factor A and the attenuation factor $\beta = \beta_N$ (the symbol N is added to β to emphasize the fact of attenuation per one chain unit). The theory allows us to express factors A and β_N through the parameters of a modified superexchange model and thus, to clarify the features of formation of the tunneling transmission. Along with the experimental data, we use strict relations between the parameters of the model. Additionally, semiphenomenological and quantum-mechanical estimates of the parameters are taken into account. Particular attention is paid to the control of conductance by anchor groups. The control is carried out in two ways. One way is associated with the coupling of terminal units to the end units of the alkane chain and additionally with the physical or chemical contact of the terminal units with the

surface atom/atoms. This is reflected in the magnitude of site-to-site coupling t_* and width parameter Γ_* (cf. Fig. 1). The second controlling mechanism is determined by the position of the terminal on-site energies $E_* - |e|V\eta_*$ and $E_* - |e|V\,(1-\eta_*)$ (cf. Fig. 2), relative to the chemical potentials of the electrodes [through the gaps (19)].

A. Near-zero bias tunneling conductance

Studies of the dependence of the tunneling current and conductance with the length of n-alkane chains anchored to the electrodes with dithiol, diamine, and dicarboxylic-acid linker groups show that the ohmic transmission regime is hold at $|V| \le 0.4$ V.[26] In the ohmic tunneling regime, the conductance is practically independent of voltage bias. In accordance with Eq. (18), this yields

$$g \simeq g_u \Phi(\beta_N, N), \quad (N = n - 1 \ge 1), \tag{20}$$

where $\beta_N = \beta(\varepsilon = \Delta E_s)$ is the zero-bias attenuation factor (per unit C–C) and

$$g_u \equiv g_{|N=1} = g_{|n=2} \tag{21}$$

is the zero-bias conductance of the symmetric molecular wire with one C–C bridging unit (two CH_2 groups). In this quantity, the contact characteristics are concentrated in the factor

$$\lambda = \sqrt{g_u/g_0} = \Gamma_e/\Delta E_s, \tag{22}$$

which is the ratio between the edge width factor $\Gamma_e = \Gamma_1(\Delta E_*) = \Gamma_N(\Delta E_*)$, Eq. (5), and the unbiased principal transmission gap ΔE_s.

The chain attenuation function $\Phi(\beta_N, N)$, Eq. (13), is not proportional to $\exp(-\beta_N N)$. However, if $\exp[-(N+1)\beta_N] \ll 1$, then

$$\Phi(\beta_N, N) \simeq (1 - e^{-2\beta_N})^2 e^{-\beta_N(N-1)}. \tag{23}$$

In the alkane chain where $\beta_N > 0.75$, form (23) is fulfilled with high accuracy already for $N = n - 1 \ge 3$. Thus, the modified superexchange model shows that one can analyze the conductance of the n-alkane wires with the use of simple expression

$$g \simeq A_{CH_2} e^{-\beta_N n}, \quad (n = N + 1 \ge 4), \tag{24}$$

if only the number of CH_2 groups in a chain is at least 4. At the same time, the correspondence between the pre-exponential factor A_{CH_2} and the superexchange factor g_u is established by the relationship

$$A_{CH_2} = 4 g_u \sinh^2 \beta_N. \tag{25}$$

From a physical point of view, it follows that

$$\Gamma_e < \Gamma_*. \tag{26}$$

Condition (26) can be violated if there is a strong chemical binding of the anchor groups X to the adjacent edge CH_2 groups of the alkane chain. In this case, the X and CH_2 groups can form extended terminal units, thus reducing the number of interior CH_2 groups of the alkane chain from n to $n-2$ (or, what is the same, the number of bridging C–C chain units from N to $\tilde{N} = N - 2$). Therefore, instead of Eq. (20), we get

$$g \simeq \tilde{g}_u \Phi(\beta_N, \tilde{N}) \quad (\tilde{N} = n - 3 \ge 1). \tag{27}$$

Here,

$$\tilde{g}_u \equiv g_{|\tilde{N}=1} = g_{|N=3} = g_{|n=4} \tag{28}$$

is the zero-bias conductance of the symmetric molecular wire with the extended terminal units $\tilde{X}$ bridged by the only interior C–C bond (two CH_2 groups). Since the function $\Phi(\beta_N, \tilde{N})$ is proportional to $\exp[-\beta_N(\tilde{N}-1)]$ for $\tilde{N} \ge 3$, then according to formula (23), conductance behavior manifests itself in the form

$$g \simeq \tilde{A}_{CH_2} e^{-\beta_N n}, \quad (n = \tilde{N} + 3 \ge 6). \tag{29}$$

In Eq. (29), the pre-exponential factor $\tilde{A}_{CH_2}$ is given by expression (25) where one has to replace g_u, Eq. (21), on $\tilde{g}_u$, Eq. (28).

As follows from the above results, analyzing the conductance with the use of formulas (24) and (29) allows one to obtain the numerical values of pre-exponential and attenuation factors A_{CH_2} ($\tilde{A}_{CH_2}$) and β_N, respectively. After that, in accordance with relationship (25), it becomes possible to estimate the conductance $g_u(\tilde{g}_u)$ of the wire with one bridging unit. Finally, using general expressions (20) and (27), obtained in the framework of the modified superexchange model, we can describe conductance of linear molecular wires with an arbitrary number of internal repeating units.

B. Key superexchange parameters

The experimental values of attenuation and contact factors (β_N and λ, respectively) are shown in Table III. The ratio of key parameters, α, is also given there. It follows from Eqs. (14) and (17) that the ratio is exclusively expressed through attenuation factor β_N,

$$\alpha \equiv \Delta E_s/2t_s = \begin{cases} (1/2)\exp(\beta_N/2), & \text{standard model}, \\ \cosh(\beta_N/2), & \text{modified model}. \end{cases} \tag{30}$$

Expressions (22) and (30) as well as the data of Tables III and IV allow one to discuss the mechanism of control of conductance by terminal units. The discussion is held in parallel with the evaluation of key and contact parameters of the modified superexchange model. Substituting $\varepsilon = \Delta E_s$ into inequalities (15) and (16), one can see that in line with the data of Table III, only inequality (15) holds. This means that the standard superexchange model is not applicable to describe tunneling through an alkane chain, regardless of which of the anchor groups (COOH, NH_2, or SH) makes contact with the electrodes. Therefore, the description below is carried out using a modified superexchange model. It was shown above that it was this model that allowed us to indicate at which length of an alkane chain one can use simple formulas (24) or (29) to analyze the experimental data.

If one knows the numerical value of at least one of the key superexchange parameters, then using the relationship between them, Eq. (30), it becomes possible to find the numerical value of

TABLE III. Factors β_N and λ as well as calculated ratio α in the standard (stnd) and modified (mdf) superexchange models.

Expt.	High conductance			Low conductance		
β_N	0.813	0.817	1.02	0.77	0.88	1.08
Λ	0.043	0.105	0.334	0.013	0.028	0.186
α stnd	0.75	0.75	0.83	0.73	0.78	0.86
α mdf	1.08	1.09	1.13	1.08	1.10	1.15
Linker	COOH	NH_2	SH	COOH	NH_2	SH

TABLE IV. Magnitude of the key parameters of the modified superexchange model, ΔE_s and t_s, the corresponding barrier parameters ΔE_0 and $m*$ (in elementary electron mass m_e), as well as the calculated contact parameters (all energy values in eV).

	High conductance			Low conductance		
ΔE_s	6.50	6.20	6.00	6.50	6.20	6.00
t_s	3.00	2.86	2.65	3.02	2.82	2.61
ΔE_0	0.50	0.66	0.71	0.46	0.56	0.64
$M*/m_e$	0.75	0.81	0.85	0.74	0.80	0.84
Γ_e	0.27	0.65	2.20	0.08	0.17	1.11
Γ_*	0.40	0.80	1.50	0.25	0.50	1.00
ΔE_*	2.68	2.53	3.14	3.68	3.96	3.61
t_*	2.20	2.39	3.79	2.10	2.30	3.79
Linker	COOH	NH_2	SH	COOH	NH_2	SH

another parameter. One important comment to be made here. Since according to Eqs. (14) and (30), the value of the attenuation factor β_N is determined by the ratio α, then the same value of β_N can be obtained using different pairs of key parameters ΔE_s and t_s satisfying the following equation: $\Delta E_s = 2t_s \cosh(\beta_N/2)$. Our choice of key parameters is based on the fact that for the alkanedithiol molecules forming the self-assembled monolayers on the polycrystalline gold substrate, the principal zero-bias gap ΔE_s is estimated at 6.3 eV and accordingly $t_s \approx 2.78$ eV.[37,39] The value of 6.3 eV follows from the condition that no resonance peaks are observed out to 1.5 V.[19] As for t_s, its value is close to the calculated values of 2.74 eV and 2.5 eV, which characterize coupling t_{C-C} between the nearest carbon atoms in graphene[68] and aromatic ring,[69,70] respectively.

From Table III, it follows that the increase in the superexchange attenuation factor β_N happens in parallel with the increase in contact factors λ, Eq. (22). This directly indicates that anchor groups affect the key superexchange parameters t_s and ΔE_s. To understand the physical reason for such an effect, we note that the experimental data were obtained under conditions where the anchoring sulfur atoms are chemically linked to both left and right electrodes. The alkane chain is thus in a more stretched position compared to when the chain is attached to the substrate on one side only. This should lead to a smaller magnitude of t_s compared to 2.78 eV. At the same time, the t_s is waited to be higher if the COOH groups are used as linkers. This is due to the fact that COOH groups do not form chemical bonds with the surfaces of the electrodes but have only physical contact with them. Thus, the structure of the alkane chain anchored to the electrode via COOH linkers is close to the structure of free chain. Therefore, the distance and orientation between the localized σ-orbitals of the neighboring C–C bonds are optimal, which leads to a higher possible value of the parameters ΔE_s and t_s. When the alkane chain is stretched due to the chemical binding of anchor groups to the electrodes, the overlap between the noted σ-orbitals decreases, resulting in a decrease in the parameter t_s and, to a lesser degree, the parameter ΔE_s. This circumstance is reflected in Table IV, which shows that t_s(COOH) > t_s(NH_2) > t_s(SH) and ΔE_s(COOH) > ΔE_s(NH_2) > ΔE_s(SH). The alteration of the key superexchange parameters leads to an alteration of the ratio $\Delta E_s/2t_s$ and, according to relation (30), the attenuation factor β_N. Thus, there is a complete correlation between the increase in α and β_N and the increase in the binding strengths of the anchoring groups COOH, NH_2, and SH on electrode's surface. This explains the dependence of the β_N on the types of anchor groups presented in Table III.

C. Apparent tunneling barrier

In the case of the alkane chains, the modified superexchange model leads to the ratio α, Eq. (30), which only slightly exceeds identity. Therefore, one can set $\alpha = 1 + \Delta E_0/2t_s$, where

$$\Delta E_0 = \Delta E_{|V=0} = \Delta E_s - 2t_s \tag{31}$$

is the zero-bias energy difference between the tunneling energy $E \simeq E_F$ and HOMO-level energy E_H (cf. definition ΔE in Fig. 2). Since condition

$$\Delta E_0 \ll 2t_s \tag{32}$$

is satisfied, then $\beta_N \approx 2\sqrt{\Delta E_0/t_s}$. Now, following the approach which was used to study the donor-acceptor electron transfer through proteins[71] and tunneling across a molecular wire,[37] we can introduce the effective electron mass,

$$m^* = \hbar^2/2t_s l_s^2. \tag{33}$$

This yields $\exp[-\beta_N(N-1)] = \exp(-\beta_B d)$, where

$$\beta_B = (2/\hbar)\sqrt{2m^*\Delta E_0} \tag{34}$$

is the attenuation factor (in $Å^{-1}$) in the barrier model. In an alkane chain, the $d = l_s(N-1)$ is attributed to the distance (in Å) between edge's C–C chain units $k = 1$ and $k = N$ (or $k = 2$ and $k = N-1$, if the edge CH_2 groups are included in the structure of extended terminal units). It follows from Eq. (34) that the ΔE_0 can be referred to the height of the apparent zero-bias rectangular barrier of width d. We note, however, that such an interpretation is possible provided that the specific condition, Eq. (32) is satisfied.

Quantum-mechanical estimations of the zero-bias gap between the HOMO and the Fermi level (in our notation ΔE_0) are a very difficult problem. Meanwhile, even a change of the gap of 0.1 eV can vary the conductance by a factor of 5.[55] Therefore, when analyzing an experiment using the attenuation factor in form (34), the barrier height ΔE_0 is considered as a fitting parameter. The same applies to zero-bias principal gap $\Delta E_s = E_F - E_{c|V=0} = \Delta E_{Ls|V=0} = \Delta E_{Rs|V=0}$ (cf. Fig. 2). The concept of a rectangular tunneling barrier is maintained as long as condition (8) is satisfied and thus, the applied voltage does not destroy the delocalization of chain orbitals (C–Cσ orbitals in the alkane chain). Assuming $\zeta = 0.2$, which well enough guarantees the applicability of the theory, one can see (cf. Fig. 3) that under the ohmic regime of nonresonant tunneling, the delocalization of the C–Cσ orbitals is conserved independently of the types of anchor groups. Therefore, a rectangular barrier can exist even at $V = 0.4$ V, if only the number of CH_2 groups in the alkane chain does not exceed 20. In the larger bias region, the collapse of delocalization occurs at much less number of bridging units. For instance, at $V = 2$ V, the delocalization is broken at $N \geq 4$ (see the inset in Fig. 3). The numerical values of the barrier heights and effective masses are

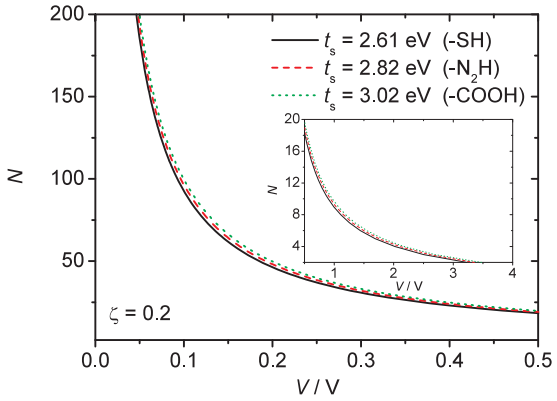

FIG. 3. The lengths of alkane chains in which the voltage bias V does not destroy the delocalization of HOMOs formed from N C–Cσ bonds.

given in Table IV. These values are determined by key parameters of the modified superexchange model via relations (31) and (33). However, the use of parameters ΔE_0 and m^* instead of ΔE_s and t_s is possible only if condition (32) is fulfilled, under which the ratio (30) does not exceed 0.2. Note that the obtained barrier heights do not exceed 1 eV, which is qualitatively consistent with the results obtained in some experiments (see, for example, the discussion in Ref. 19) and quantum-mechanical estimations.[22] For the effective mass of about 0.8 m_e, it corresponds to a "heavy" hole mass in the valence (HOMO) band.[72]

D. Contact parameters

After evaluating the key superexchange parameters ΔE_s and t_s, the values of which are given in Table IV, it becomes possible to estimate the edge width factors. To do this, note that according to Eq. (22),

$$\Gamma_e = \lambda \Delta E_s. \tag{35}$$

Therefore, with the use of experimental data for λ given in Table III, we come to the possible magnitude of the edge width factor Γ_e.

In accordance with definition (5), the factor Γ_e is proportional to the width parameter Γ_* characterizing the broadening of the orbital energy of the terminal unit [cf. Eq. (5)]. Therefore, the greater the binding strength, the greater the Γ_*, and with it, Γ_e. This is in complete accordance with the previously made conclusion.[26] To estimate the Γ_*, let us not that in accord with the quantum-mechanical studies, the Au s-orbital and the N lone pair form an antibonding hybrid orbital,[64] which can be associated with the HOMO of wire's terminal unit. It is known that the S–Au bond is stronger than the Au–N bond.[73] Therefore, a similar hybridization also becomes possible between Au and S atoms.[47] Using the News-Anderson model,[74] we obtain the following expression for the broadening of Au–S HOMO: $\Gamma_* \approx (1/2)t_{\text{Au-S}}^2/t_{\text{Au-Au}}$. (Factor 1/2 supposes that the weights of Au and S atomic orbitals are approximately equal to each other in the hybrid Au–S HOMO.) Considering that Au–Au and Au–S couplings are equal, respectively, to $t_{\text{Au-Au}} \approx 2.65$ eV and $t_{\text{Au-S}} \approx 2.00$ eV,[47] one can see that the broadening of energy level associated with the SH linker is Γ_*(SH) $\approx$ 1.5 eV. The Au–N contact and even more the contact of COOH with the gold surface, are not too strong as Au–S contact. For carrying out rough estimates, we assume that Γ_*(SH): Γ_*(NH$_2$): Γ_*(COOH) $\approx$ 1:0.50:0.25. Width parameter Γ_* strongly depends on the large variability to the anchor-electrode contact geometry[7,16,55] and, thus, we use Γ_* as a fitting parameter, setting Γ_*(SH) = 1.5 (1.0) eV for the high (low) conductance. Now, using expression (5) and taking into account inequality $(\Gamma_*/2\Delta E_*)^2 \ll 1$ which is valid for near zero-bias tunneling, we arrive at the relation

$$t_*/\Delta E_* \simeq (\Gamma_e/\Gamma_*)^{1/2}. \tag{36}$$

If the value of transmission gap ΔE_* is known, then relation (36) allows us to estimate the coupling t_s of terminal units X to the adjacent edge units of the alkane chain. For linkers SH, NH$_2$, and COOH, the gaps ΔE_* are less than the principal transmission gap ΔE_s but

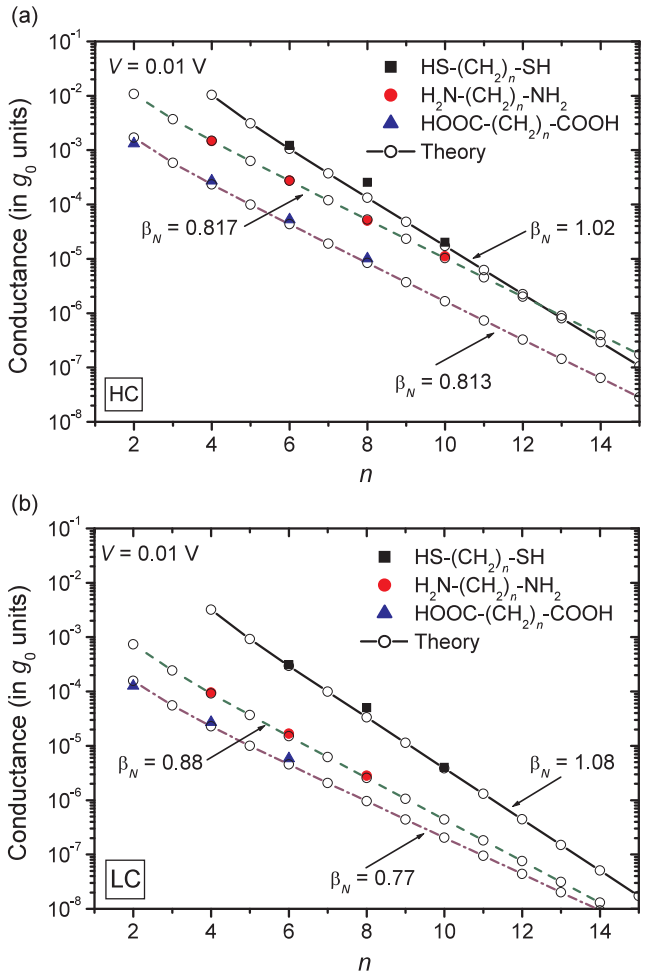

FIG. 4. High (a) and low (b) near zero-bias conductance of X–$(CH_2)_n$–X molecular wires with different anchor groups X. The point symbols represent the data adopted from the experiment plots[26] as well as from theoretical calculations performed with the parameters presented in Table IV following Eq. (18). The theory predicts a deviation from purely exponential behavior for short alkanes anchored by NH$_2$ and especially SH groups. Deviations may be large for the bridging chains with $\beta_N < 0.6$.

exceed the HOMO-Fermi level gap ΔE_0. This follows from the fact that energies of the lone pair orbitals localized on the sulfur and oxygen atoms are positioned above the orbital energy of the C–C bond.[60] The precise magnitude of gap ΔE_* is unknown, and therefore we take this as the fitting parameter. The data on the parameters, which in the framework of the modified superexchange model characterize the high and low conductance of terminated alkane chains, are presented in Table IV. The data show that for linker SH, the edge width factor Γ_e is so great that condition (26) is not fulfilled. Thus, there is reason to assume that the chemical bonding of the anchor sulfur atom with the gold electrode can bring to the formation of the hybrid Au–S–C structure and, thus, to expand terminal units from Au–S to Au–S–CH_2. Under this situation, the number of interior CH_2 units in the wire S–$(CH_2)_n$–S decreases and the wire itself can be represented as the (S–CH_2)–$(CH_2)_{n-2}$–(CH_2–S) structure. The conductance of such a structure, a regular range of which includes only $n \geq 6$ CH_2 groups (or, equivalently, $N \geq 5$ C–C bonds), is given by Eq. (29).

E. Compliance with experimental results

Figure 4 shows that the experimental point symbols well reflect an exponential decrease in conductance, described by formulas (24) and (29). However, more accurate formulas (20) and (27) assume the deviation from the exponential law at $n < 4$ and $n < 6$ for linkers COOH (NH_2) and SH, respectively. The same conclusion follows from the general formula of the modified superexchange model, Eq. (18), which, under the ohmic regime of an electron tunneling transmission, reduces to forms (24) and (29). Deviation from the exponential behavior for short bridging chains means that, generally, if the conductance is analyzed with expression $g = A\exp(-\beta d)$, where $\beta = \beta_N l_s^{-1}$, then the magnitude of the pre-exponential factor for a short bridging chain has to differ from the magnitude that is determined via approximation $A = g_{|d\to 0}$. For the terminated alkane chain, this conclusion follows directly from asymptotic formula (23) if one takes into account the fact that $d = l_s(N-1) = l_s(n-2)$ (at $n > 4$) and $d = l_s(\tilde{N}-1) = l_s(n-4)$ (at $n > 6$) are the tunneling distances within the interior range of wires with the anchors X = COOH (NH_2) and X = SH, respectively. Thus, a pure exponential attenuation can appear if only the minimal width of the rectangular barrier is $d \geq 3l_s$. For short alkane chains with $\beta_N > 0.75$, the deviation of attenuation from the exponential one is not large. However, for bridging chains, where $\beta_N < 0.6$, the deviation can be appreciable.

IV. CONCLUSION

The main goal of this work was to elucidate the features of the physical mechanisms controlling the formation of a bridge-mediated tunneling transmission. In a molecular nanowire, such a control is regulated by the energy and structural properties of terminal and interior units of the wire as well as the interface. The experimental results were analyzed using a modified superexchange model. The model makes it possible to obtain analytical formulas that have well-defined areas of applicability. Unlike the standard (McConnell) superexchange model, the modified model has fewer restrictions on the ratio $\alpha = \Delta E_s/2t_s$ between its key parameters ΔE_s and t_s. As follows from inequalities (15) and (16) with $\varepsilon = \Delta E_s$, the standard model can describe nonresonant conductance under the condition of $\alpha^2 \gg 1$, whereas for the application of the modified model, it suffices to comply with the inequality $\alpha > 1$. Therefore, a modified superexchange model has a much wider area of its applicability. The capabilities of the model were demonstrated when analyzing the tunneling conductance of molecular wires comprising *n*-alkane chains anchored to electrodes by COOH, NH_2, and SH linkers.

Among the results of general physical significance, we note the following:

1. Our studies lead to the conclusion that the results obtained in the framework of the standard (McConnell) superexchange and the flat-barrier (Simmons) models follow as different limiting cases from the modified superexchange model. For instance, the decay coefficients (17) and (34) appear as the limiting values of the attenuation factor (14). This conclusion can be assigned to a new and important result, which, as to our knowledge, has not been previously reported.
2. The estimates show that the standard superexchange model can be used if $\alpha^2 > 10$. This inequality is realized at $\beta_N > 3.7$. As to the flat-barrier model, its application is restricted by the range $1 < \alpha < 1.2$ so that the model works at $\beta_N < 1.2$. Physically, the difference in the domains of applicability of the models is due to the fact that the barrier model reflects a participation of delocalized virtual orbitals of the bridging chain, whose energy is not too far from the Fermi levels (i.e., at $\Delta E \ll 2t_s$, see Fig. 2). In contrast, the standard superexchange model involves the participation of localized or weakly delocalized virtual orbitals with energies positioned far from Fermi levels (i.e., at $\Delta E \gg 2t_s$). Thus, both models have specific strictly different areas of applicability. The modified model does not have such limitations. It works at $\beta_N > 0$ and thus, can be applied to analyze the tunneling conductance of molecular wires containing the bridging chains not only with saturated but also with unsaturated bonds. This is a new result concerning the application of the physical models to analyze the experimental data.
3. From a practical point of view, an important result is a general analytical formula [Eq. (18)]. It allows analyzing the tunneling conductance of a terminated linear wire under conditions when the voltage bias does not destroy the delocalization of the orbitals belonging to the interior range of the wire (i.e., the chain of *N* repeating units). With a small voltage bias, the general formula goes into simpler formulas (20) and (27). The latter have the corresponding asymptotic expressions (24) and (29), in which the factors $A(\tilde{A})$ and β_N are expressed in terms of the parameters of the superexchange model. All formulas have strictly fixed limits of applicability and are therefore particularly convenient for processing experimental data. For alkane chains, the gaps $\Delta E_s = \Delta E_{c|V=0}$ and $\Delta E_0 = \Delta E_{|V=0}$ are defined as the distance between the energy of Fermi level (E_F) and energy position of the corresponding localized C–Cσ orbitals ($E_s = E_{c|V=0}$) and the delocalized HOMO (E_H), Fig. 2, while t_s characterizes the coupling between adjacent repeating C–C units, Fig. 1. As follows from the data of Table III, the estimation of the conductance with the use of the standard superexchange model brings to inequality $\alpha < 1$, which contradicts condition $\alpha^2 \gg 1$ of the applicability of the model. This indicates that the standard model is not applicable to the description of nonresonant tunneling through the alkane

chains. In contrast, the condition $\alpha > 1$ of the applicability of the modified superexchange model is well satisfied. Based on the experimental data on the attenuation of high and low conductance, the key parameters of the modified superexchange model are estimated as well as the parameters characterize the contact of wires X–$(CH_2)_n$–X with electrodes through anchor groups COOH, NH_2, and SH (Table IV). Moreover, bearing in mind the fact that $\alpha = 1 + \kappa$ and $\kappa = \Delta E_0/2t_s \ll 1$, it becomes possible to introduce the key parameters of the barrier model ΔE_0 and m^*, Eqs. (31) and (33), respectively. Magnitudes of these parameters are also presented in Table IV.

4. Once more important property of the modified superexchange model is that the model shows a deviation of conduction attenuation from the exponential law for short bridging chains. This conclusion follows from the fact that the chain attenuation function, Eq. (13), manifests its exponential behavior, Eq. (23), only if the number of chain units exceeds a certain value. This deviation is not large for alkane chains, but it could be well noticeable in molecular wires, where $\beta_N < 0.6$.
5. An additional effect is associated with a possible hybridization of anchor groups and adjacent terminal chain units, when the extension of terminal groups becomes possible. From the modified superexchange model, it follows that the extension is reflected in the disarrangement of inequality (26). The estimations show that in the case of alkane chain as the bridging structure, the extension of wire's terminal units and, simultaneously, the shortening of the interior range of the wire become possible if the chain is chemically anchored to both gold surfaces by the SH linkers.

In the present work, the zero-bias conductance of molecular wires was analyzed, which made it possible to obtain the provisional estimates of the parameters. More accurate estimates can be made with the use of data on the conductance of the same molecular wires under the voltage biases that bring to deviation of a tunneling current from the ohmic regime. The modified superexchange model also works in this case, if only $\alpha_r = \Delta E_{rs}/2t_s = 1 + \kappa_r > 1$ ($r = L, R$). Dependence of the ratio α_r on the voltage bias is comprised of the principal transmission gaps ΔE_{rs}, Eq. (12). The tunneling electron current and conductance can be analyzed with respective equations (11) and (18). At the same time, attention should be paid to the fact that the concept of a rectangular barrier is conserved if only the quantity $\kappa_r = \kappa - (|e|V/2t_s)(\delta_{r,L} - \delta_{r,R})$ is in the interval $0 < \kappa_r \ll 1$ and, additionally, the delocalization condition, Eq. (8) is hold.

Summarizing the results, one can conclude that the modified superexchange model can be used as an appropriate physical model that allows us to obtain rigorous analytic results suitable for the analysis of tunneling processes in molecular wires of different origins. In parallel, it becomes possible to clarify the physical mechanisms of tunneling transmission in terms such as energy gaps and couplings that are more appropriate for molecular junctions than terms of solid-state electronics (height and width of a rectangular barrier and effective tunneling mass).

ACKNOWLEDGMENTS

E.G.P. and E.V.S. acknowledge the support from the NAS Ukraine via Project No. 0116U002067. V.S. acknowledges the support from the MSU Global Education Grant. This project has received funding from the European Union's Horizon 2020 research and innovation programme under the Marie Sklodowska-Curie Grant Agreement Nos. NANOGUARD2AR 690968 (S.L.) and ENGIMA 778072 (V.V.G. and A.V.R.).

REFERENCES

[1] *Molecular Electronic Devices*, edited by F. L. Carter (Marcel Dekker, New York, USA, 1982).
[2] A. Nitzan, Annu. Rev. Phys. Chem. **52**, 681–750 (2001).
[3] R. L. McCreery, Chem. Mater. **16**, 4477–4496 (2004).
[4] B. K. Pathem, S. A. Claridge, Y. B. Zheng, and P. S. Weiss, Annu. Rev. Phys. Chem. **64**, 605–630 (2013).
[5] S. V. Aradhya and L. Venkataraman, Nat. Nanotechnol. **8**, 399–410 (2013).
[6] K. V. Raman, Appl. Phys. Rev. **1**, 031101 (2014).
[7] D. Xiang, X. Wang, X. Jia, T. Lee, and X. Guo, Chem. Rev. **116**, 4318–4440 (2016).
[8] J. C. Cuevas and E. Scheer, *Molecular Electronics: An Introduction in Theory and Experiment*, 2nd ed. (World Scientific, 2017), Vol. 15.
[9] M. A. Ratner, Nat. Nanotechnol. **8**, 378–381 (2013).
[10] M. Baghbanzadeh, C. M. Bowers, D. Rappoport, T. Zaba, M. Gonidec, M. H. Al-Sayah, P. Cyganik, A. Aspuru-Guzik, and G. M. Whitesides, Angew. Chem., Int. Ed. **54**, 14743–14747 (2015).
[11] C. A. Nijhuis, W. F. Reus, A. C. Siegel, and G. M. Whitetesides, J. Am. Chem. Soc. **133**, 15397–15411 (2011).
[12] Z. Li, M. Smeu, S. Afsari, Y. Hing, M. A. Ratner, and E. Borguet, Angew. Chem. **126**, 1116–1120 (2014).
[13] J. L. Zhang, J. Q. Zhong, J. D. Lin, W. P. Hu, K. Wu, G. Q. Xu, A. T. Wee, and W. Chen, Chem. Soc. Rev. **44**, 2998–3022 (2015).
[14] B. Cappozzi, J. Xia, O. Adak, E. J. Dell, and Z. E. Lin, Nat. Nanotechnol. **10**, 522–527 (2015).
[15] R. M. Metzger, Chem. Rev. **115**, 5056–5115 (2015).
[16] T. A. Su, M. Neupane, M. L. Steigerwald, L. Venkataraman, and C. Nuckolls, Nat. Rev. Mater. **1**, 16002 (2016).
[17] L. Lafferentz, F. Ample, H. Yu, C. Joachim, and L. Grill, Science **323**, 1193–1197 (2009).
[18] F. Lortsher, Nat. Nanotechnol. **8**, 381–384 (2013).
[19] V. B. Engelkes, J. M. Beebe, and C. D. Friesbie, J. Am. Chem. Soc. **126**, 14287–14296 (2004).
[20] K.-C. Liao, L.-Y. Hsu, C. M. Bowers, H. Rabitz, and G. M. Whitesides, J. Am. Chem. Soc. **137**, 5948–5954 (2015).
[21] F. C. Simeone, H. J. Yoon, M. M. Thuo, J. R. Barber, B. Smith, and G. M. Whitesides, J. Am. Chem. Soc. **135**, 18131–18144 (2013).
[22] J. K. Tomfohr and O. F. Sankey, Phys. Rev. B **65**, 245105 (2002).
[23] F. Picaud, A. Smogunov, A. D. Corso, and E. Tossati, J. Phys.: Condens. Matter **15**, 3731–3740 (2003).
[24] J. K. Tomfohr and O. F. Sankey, J. Chem. Phys. **120**, 1542–1554 (2004).
[25] S. Yi. Quek, H. J. Choi, S. G. Louie, and J. B. Neaton, Nano Lett. **9**, 3949–3953 (2009).
[26] F. Chen, X. Li, J. Hihath, Z. Huang, and N. Tao, J. Am. Chem. Soc. **128**, 15874–15881 (2006).
[27] C. M. Kim and J. J. Bechhoefer, J. Chem. Phys. **138**, 014707 (2013).
[28] J. G. Simmons, J. Appl. Phys. **34**, 1793–1803 (1963).
[29] H. M. McConnell, J. Phys. Chem. **35**, 508–515 (1961).
[30] J. Selzer, A. Salomon, and D. Cahen, J. Phys. Chem. B **106**, 10432–10439 (2002).
[31] X. D. Cui, A. Primak, X. Zarate, J. Tomfohr, O. F. Sankey, A. L. Moore, T. A. Moore, D. Gust, L. A. Nagahara, and S. M. Lindsay, J. Phys. Chem. B **106**, 8609–8614 (2002).
[32] H. B. Akkerman, R. C. G. Naber, B. Jongbloed, P. A. van Hal, P. W. M. Blom, D. M. de Leeuw, and B. de Boer, Proc. Natl. Acad. Sci. U. S. A. **104**, 11161–11166 (2007).

[33]E. H. Huisman, C. M. Guedon, B. van Wees, and S. J. van der Molen, Nano Lett. **9**, 3909–3913 (2009).
[34]I. Bâldea and H. Köppel, Phys. Status Solidi B **249**, 1791–1804 (2012).
[35]V. Mujica, M. Kemp, and M. A. Ratner, J. Chem. Phys. **101**, 6856–6864 (1994).
[36]J. W. Evenson and M. Karplus, J. Chem. Phys. **96**, 5272–5278 (1992).
[37]E. G. Petrov, JETP Lett. **108**, 302–311 (2018).
[38]E. G. Petrov, Phys. Status Solidi B **256**, 1900092 (2019).
[39]J. Hihath and T. Nongjian, Semicond. Sci. Technol. **29**, 054007 (2014).
[40]X. D. Cui, X. Zarate, J. Tomfohr, O. F. Sankey, A. Primak, A. L. Moore, T. A. Moore, D. Gust, D. Harris, and S. M. Lindsay, Nanotechnology **13**, 5–14 (2002).
[41]M. A. Rampi and G. M. Whitesides, Chem. Phys. **281**, 373–391 (2002).
[42]J. Jortner, M. Bixon, A. A. Voityuk, and N. Rösch, J. Phys. Chem. A **106**, 7599–7606 (2002).
[43]C. R. Treadway, M. G. Hill, and J. K. Barton, Chem. Phys. **281**, 409–428 (2002).
[44]E. G. Petrov, Ya. R. Zelinskyy, V. May, and P. Hänggi, J. Chem. Phys. **127**, 084709 (2007).
[45]M.-J. Huang, L.-Y. Hsu, M.-D. Fu, S.-T. Chuang, F.-W. Tien, and C.-H. Chen, J. Am. Chem. Soc. **136**, 1832–1841 (2014).
[46]S. Datta, *Electronic Transport in Mesoscopic Systems* (Cambridge University Press, Cambridge, UK, 1995).
[47]W. Tian, S. Datta, S. Hong, R. Reifenberger, J. I. Henderson, and C. P. Kubiak, J. Chem. Phys. **109**, 2874–2882 (1998).
[48]I. Baldea, Phys. Chem. Chem. Phys. **19**, 11759–11770 (2017).
[49]V. Mujica, M. Kemp, and M. A. Ratner, J. Chem. Phys. **101**, 6849–6855 (1994).
[50]E. G. Petrov, I. S. Tolokh, A. A. Demidenko, and V. V. Gorbach, Chem. Phys. **193**, 237–253 (1995).
[51]V. V. Priyadarshy, S. S. Skourtis, S. M. Risser, and D. N. Beratan, J. Chem. Phys. **104**, 9473–9481 (1996).
[52]J. R. Widawsky, W. Chen, H. Vazquez, T. Kim, R. Breslow, M. S. Hyberstein, and L. Venkataraman, Nano Lett. **13**, 2889–2894 (2013).
[53]L.-Y. Hsu and H. Rabitz, J. Chem. Phys. **145**, 234702 (2016).
[54]N. A. Zimbovskaya, J. Chem. Phys. **146**, 184302 (2017).
[55]S. N. Yaliraki, M. Kemp, and M. A. Ratner, J. Am. Chem. Soc. **121**, 3428–3434 (1999).
[56]M. Frei, S. V. Aradhya, M. S. Hybersen, and L. Venkataraman, J. Am. Chem. Soc. **134**, 4003–4006 (2012).
[57]V. Mujica, A. E. Roitberg, and M. Ratner, J. Chem. Phys. **112**, 6834–6839 (2000).
[58]A. S. Davydov and Yu. B. Gaididey, Phys. Status Solidi B **132**, 189–201 (1985).
[59]E. Wierzbinski, X. Yin, K. Werling, and D. H. Waldeck, J. Phys. Chem. B **117**, 4431–4441 (2012).
[60]M. Baghbanzadeh, C. M. Bowers, D. Rappoport, T. Zaba, L. Yuan, K. Kang, K.-C. Liao, M. Gonidec, P. Rothemund, P. Cyganik, A. Aspuru-Guzik, and G. M. Whitesides, J. Am. Chem. Soc. **139**, 7624–7631 (2017).
[61]J. M. Beebe, V. B. Engelkes, L. L. Miller, and C. D. Frisbie, J. Am. Chem. Soc. **124**, 11268–11269 (2002).
[62]L. A. Curtiss and C. A. Naleway, Chem. Phys. **176**, 387–405 (1993).
[63]B. Kim, J. M. Beebe, Y. Jun, X.-Y. Zhu, and C. D. Friesbie, J. Am. Chem. Soc. **128**, 4970–4971 (2006).
[64]L. Venhataraman, L. Klane, I. W. Tam, C. Nuckolls, C. Hybertsen, and M. L. Steigerwald, Nano Lett. **6**, 458–462 (2006).
[65]Y. S. Park, A. C. Walley, M. Kamenetska, M. L. Steigerwald, M. S. Hybertsen, C. Nuckolls, and L. Venhataraman, J. Am. Chem. Soc. **129**, 15768–15769 (2007).
[66]S. V. Aradhya, M. Frei, M. S. Hybertsen, and L. Venkataraman, Nat. Mater. **11**, 872–876 (2012).
[67]S. S. Skourtis and S. Mukamel, Chem. Phys. **197**, 367–388 (1995).
[68]R. Kundu, Mod. Phys. Lett. B **25**, 163–173 (2011).
[69]W. P. Su, J. R. Schrieffer, and A. J. Heeger, Phys. Rev. B **22**, 2099–2111 (1980).
[70]I. Bâldea, Phys. Chem. Chem. Phys. **17**, 20217–20230 (2015).
[71]E. G. Petrov, Int. J. Quantum Chem. **16**, 133–152 (1979).
[72]S. Adachi, *GaAs and Related Materials: Bulk Semiconducting and Superlattice Properties* (World Scientific, Singapore, 1994).
[73]D. Q. Xu and N. J. Tao, Science **301**, 1221–1223 (2003).
[74]D. M. Newns, Phys. Rev. **178**, 1123–1135 (1969).